

Cell Reports, Volume 39

Supplemental information

**Critical examination of Ptbp1-mediated
glia-to-neuron conversion in the mouse retina**

Ye Xie, Jing Zhou, and Bo Chen

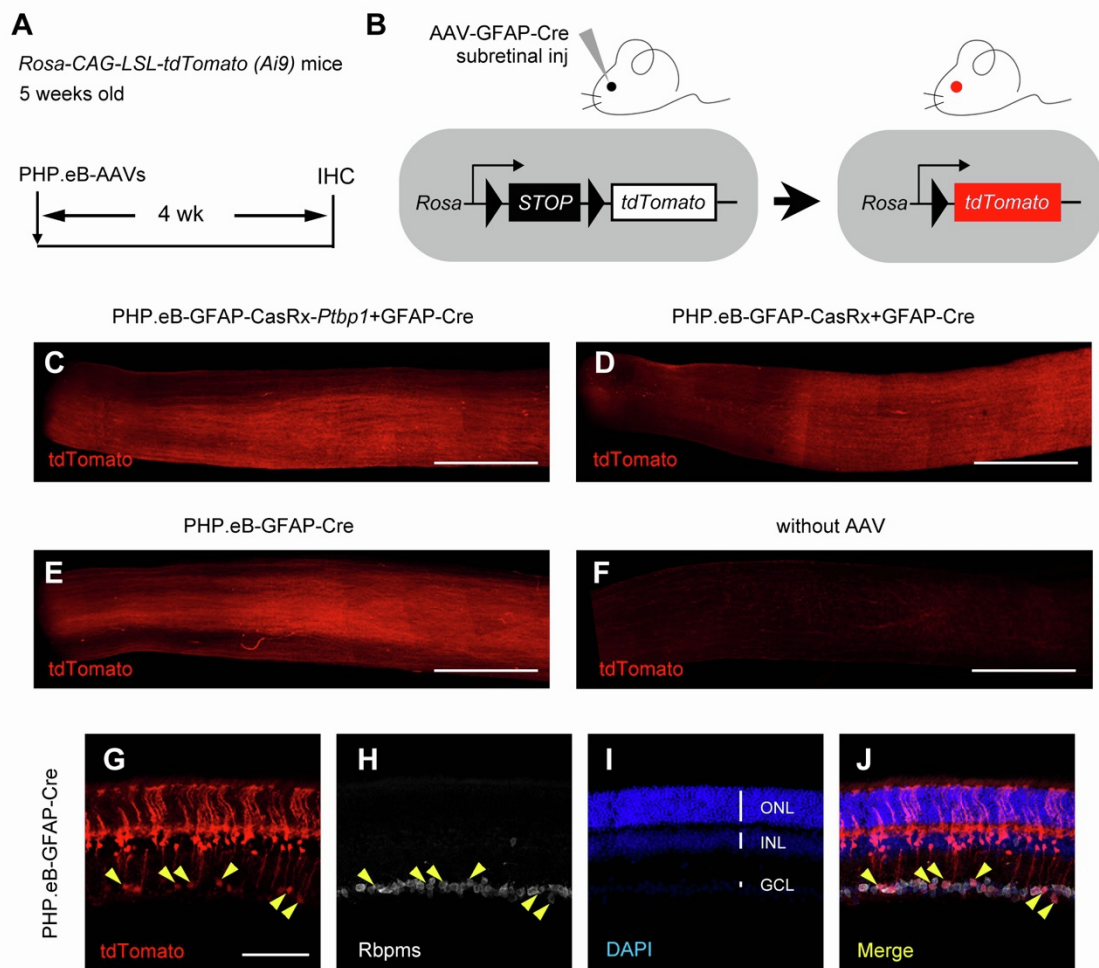


Figure S1. AAV-mediated Cre recombination labels axons from endogenous RGCs, related to Figure 1

(A) Experimental design for testing MG-to-RGC conversion and axon regeneration. Subretinal injection of PHP.eB-AAVs were performed in Rosa-CAG-LSL-tdTomato (Ai9) reporter mice at 5 weeks of age, followed by immunohistochemistry analysis using the pan-RGC marker RBPMS at 4 weeks after AAV injection. IHC, immunohistochemistry.

(B) Schematic illustration showing that AAV-GFAP-Cre subretinal injection results in tdTomato expression after Cre-dependent recombination in Ai9 reporter mice.

(C) Confocal images showing tdTomato-labeled axons in the optic nerve after injection of PHP.eB-GFAP-CasRx-*Ptbp1* (*Ptbp1* downregulation) and GFAP-Cre. Experiments were independently repeated 4 times with similar results. Scale bar, 500 μm .

(D) Confocal images showing tdTomato-labeled axons in the optic nerve after injection of PHP.eB-GFAP-CasRx (Control) and GFAP-Cre. Experiments were independently repeated 4 times with similar results. Scale bar, 500 μm .

(E) Confocal images showing tdTomato-labeled axons in the optic nerve after injection of PHP.eB-GFAP-Cre only. Experiments were independently repeated 4 times with similar results. Scale bar, 500 μm .

(F) Confocal images showing no detection of tdTomato-labeled axons in the optic nerve without AAV injection. Experiments were independently repeated 3 times with similar results. Scale bar, 500 μm .

(G-J) Confocal images showing expression of tdTomato and RBPMS immunohistochemistry in retinas receiving PHP.eB-GFAP-Cre only. Yellow arrowheads: tdTomato labeled cells were RBPMS positive in the GCL. Scale bar, 100 μm . ONL, outer nuclear layer. INL, inner nuclear layer. GCL, ganglion cell layer.

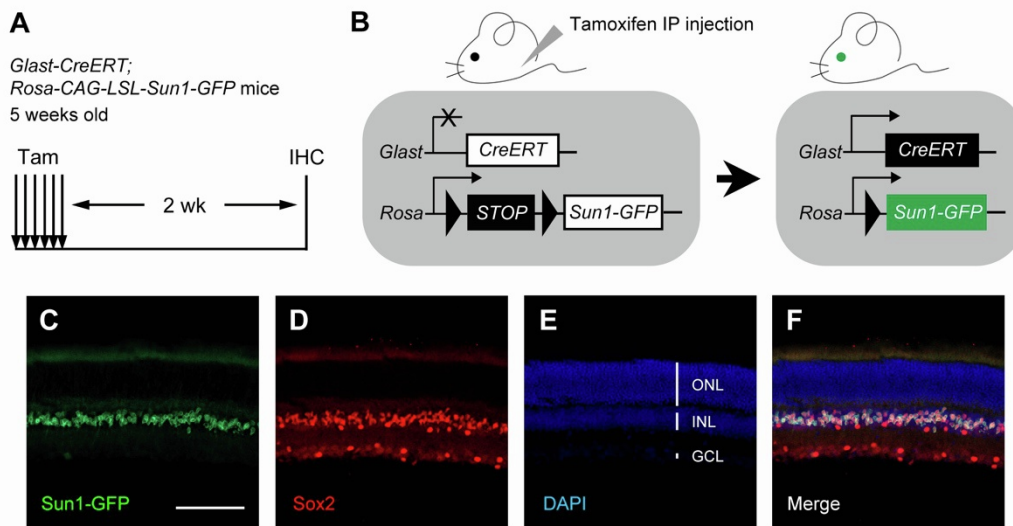


Figure S2. Generation of Sun1-GFP fate mapping mice for lineage tracing MG, related to Figure 2-4

(A) Experimental design for generating Sun1-GFP fate mapping mice by crossing the *Glax-CreERT* line with the *Rosa-CAG-LSL-Sun1-GFP* reporter line. Immunohistochemistry analysis was performed at 2 weeks after 6 consecutive daily tamoxifen IP injections in the Sun1-GFP fate mapping mice. IHC, immunohistochemistry.

(B) Schematic illustration showing that tamoxifen-induced Cre recombination results in genetic labeling of MG with Sun1-GFP expression.

(C-F) Confocal images showing that Sun1-GFP labeled MG were immunoreactive for the MG nuclear marker Sox2. Scale bar, 100 μm .

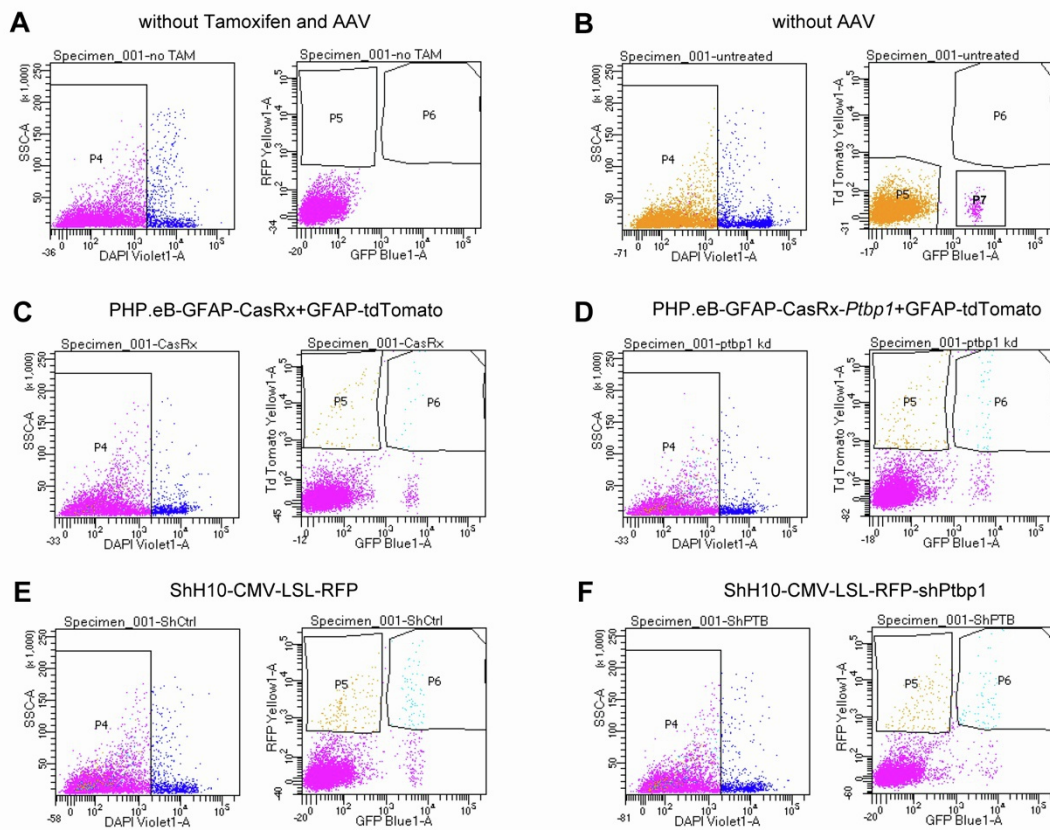


Figure S3. Fluorescence-activated cell sorting (FACS) of MG in the retinas of Sun1-GFP fate mapping mice, related to Figure 2 and 3

(A) *Glast-CreERT; Rosa-CAG-LSL-Sun1-GFP* mice (Sun1-GFP fate mapping without tamoxifen and AAV injection) were used as a gating control for FACS.

(B) FACS of Sun1-GFP⁺ MG (P7) from tamoxifen-induced Sun1-GFP fate mapping mice without AAV injection.

(C) FACS of tdTomato⁺Sun1-GFP⁺ cells (P6) from tamoxifen-induced Sun1-GFP fate mapping mice receiving PHP.eB-GFAP-CasRx and GFAP-tdTomato.

(D) FACS of tdTomato⁺Sun1-GFP⁺ cells (P6) from tamoxifen-induced Sun1-GFP fate mapping mice receiving PHP.eB-GFAP-CasRx-*Ptbp1* and GFAP-tdTomato.

(E) FACS of RFP⁺Sun1-GFP⁺ cells (P6) from tamoxifen-induced Sun1-GFP fate mapping mice receiving ShH10-CMV-LSL-RFP.

(F) FACS of RFP⁺Sun1-GFP⁺ cells (P6) from tamoxifen-induced Sun1-GFP fate mapping mice receiving ShH10-CMV-LSL-RFP-sh*Ptbp1*.

(A-F) DAPI was used as a viability dye to exclude the dead cells. P4 represents live cells used for sorting. 3-5 retinas were used in each group.

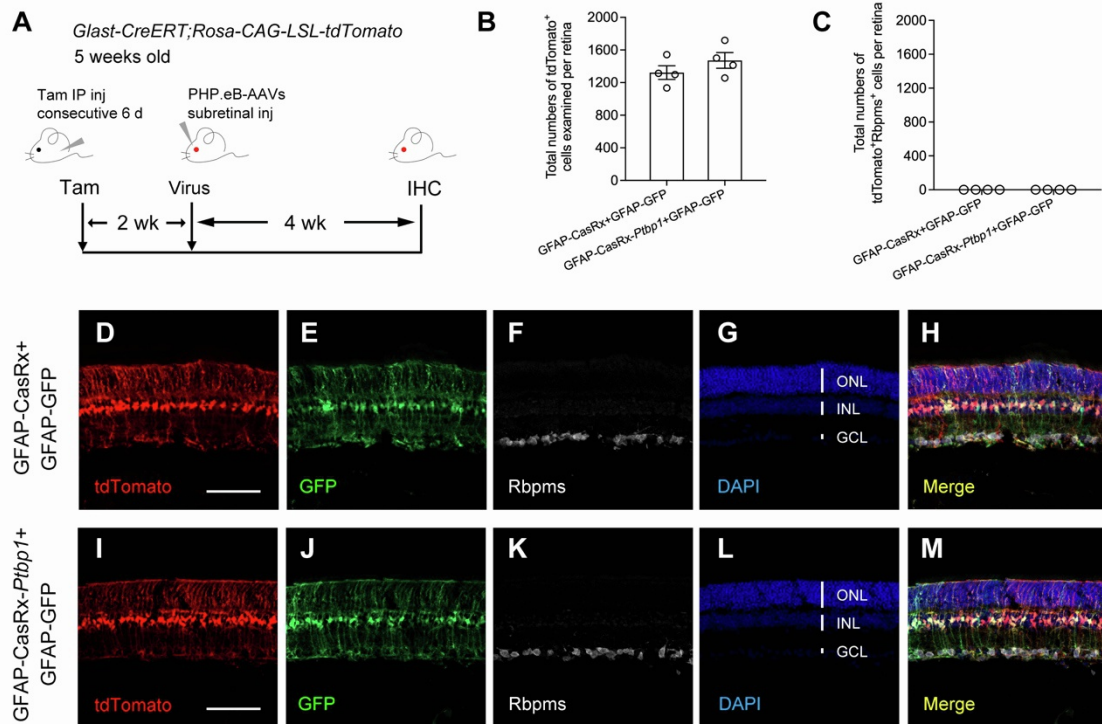


Figure S4. *Ptbp1* downregulation by CRISPR-CasRx fails to convert MG into RGCs in tdTomato fate mapping (*Glast-CreERT;Rosa-CAG-LSL-tdTomato*) mice, related to Figure 2

(A) Experimental design for testing MG-to-RGC conversion in tdTomato fate mapping mice. Subretinal injection of PHP.eB-AAVs were performed in tdTomato fate mapping mice receiving tamoxifen-induced labeling of MG at 5 weeks of age, followed by immunohistochemistry analysis using the pan-RGC marker RBPMS were performed at 4 weeks after AAV injection. IHC, immunohistochemistry.

(B) Total numbers of tdTomato labeled MG examined in retinas 4 weeks after receiving GFAP-GFP (an infection marker), together with GFAP-CasRx (control) or GFAP-CasRx-*Ptbp1* (*Ptbp1* downregulation).

(C) Total numbers of tdTomato labeled MG that were also immunoreactive for the pan-RGC marker RBPMS per retina after *Ptbp1* downregulation.

(D-H) Confocal images showing expression of tdTomato and RBPMS immunohistochemistry in retinas receiving GFAP-CasRx and GFAP-GFP.

(I-M) Confocal images showing expression of tdTomato and RBPMS immunohistochemistry in retinas receiving GFAP-CasRx-*Ptbp1* and GFAP-GFP.

(I-M) Scale bar, 100 μ m. ONL, outer nuclear layer. INL, inner nuclear layer. GCL, ganglion cell layer.

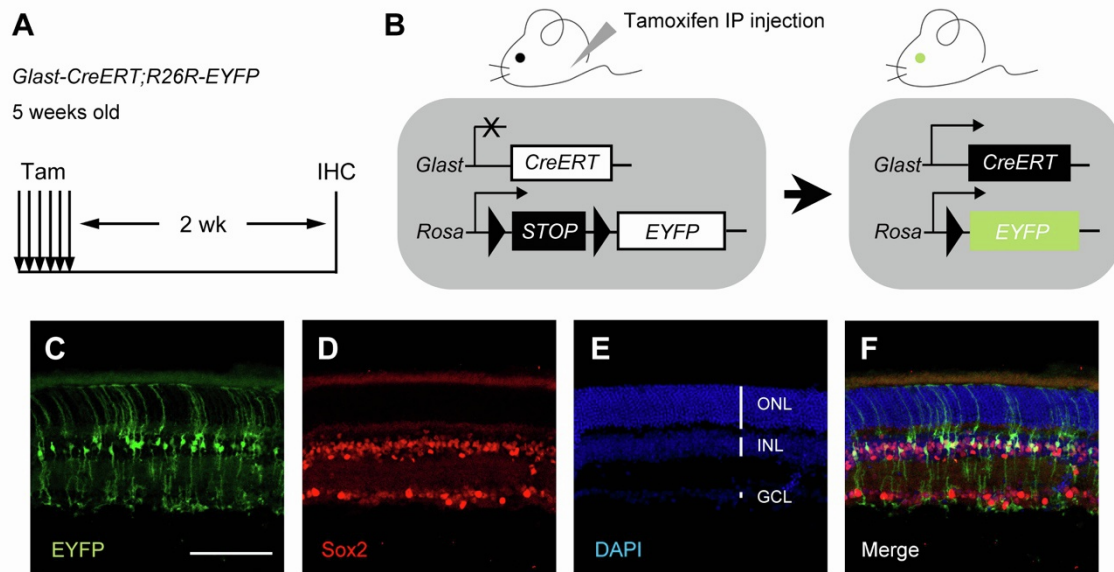


Figure S5. Generation of EYFP fate mapping mice for lineage tracing MG, related to Figure 2 and 3

(A) Experimental design for generating EYFP fate mapping mice by crossing the *Glaxt-CreERT* line with the *R26R-EYFP* reporter line. Immunohistochemistry analysis was performed at 2 weeks after 6 consecutive daily tamoxifen IP injections in the EYFP fate mapping mice. IHC, immunohistochemistry.

(B) Schematic illustration showing that tamoxifen-induced Cre recombination results in genetic labeling of MG with EYFP expression.

(C-F) Confocal images showing that EYFP labeled MG were immunoreactive for the MG nuclear marker Sox2. Scale bar, 100 μm .

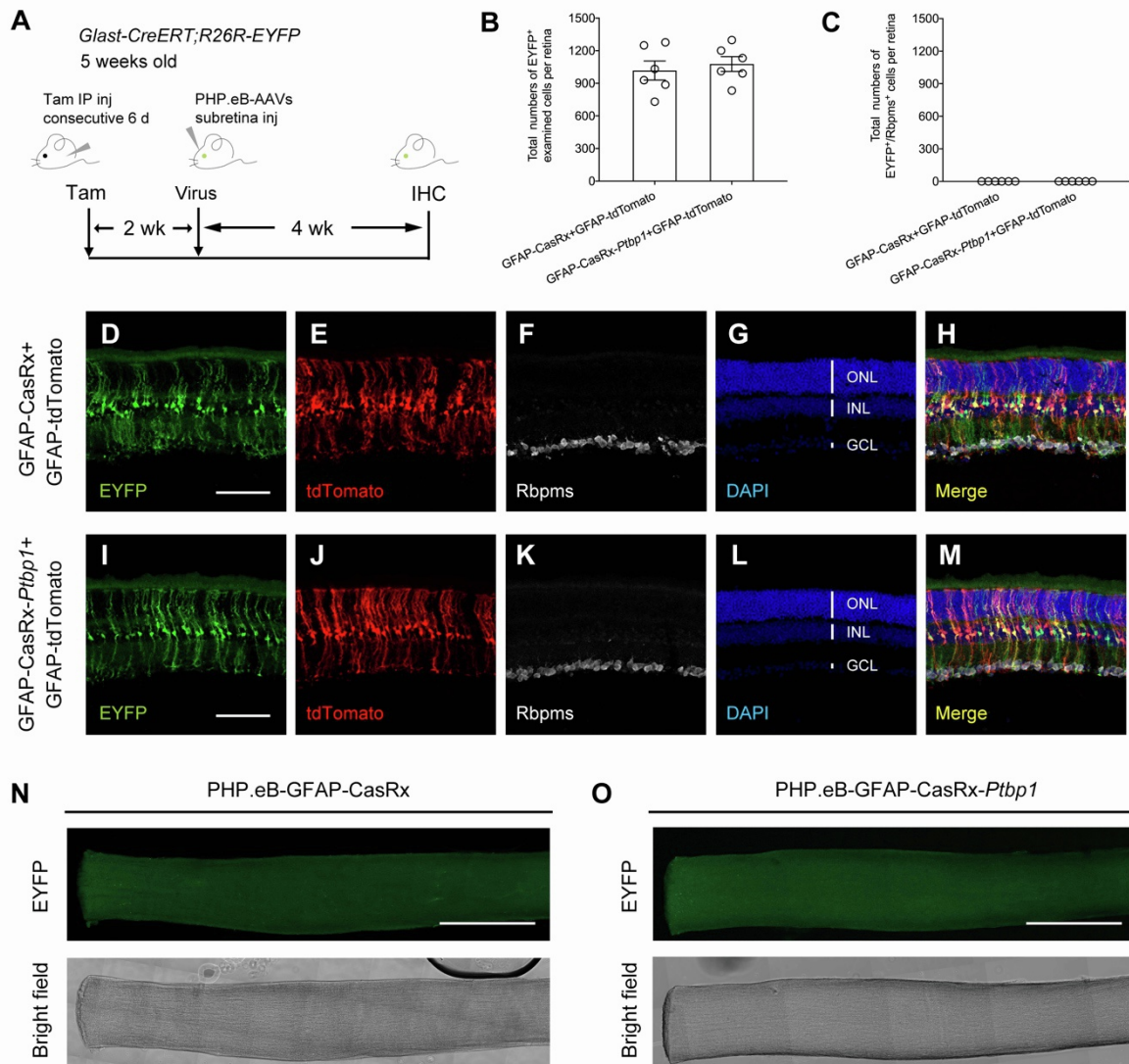


Figure S6. *Ptbp1* downregulation by CRISPR-CasRx fails to convert MG into RGCs in EYFP fate mapping (*Glast-CreERT;R26R-EYFP*) mice, related to Figure 2

(A) Experimental design for testing MG-to-RGC conversion in EYFP fate mapping mice. Subretinal injection of PHP.eB-AAVs were performed in EYFP fate mapping mice receiving tamoxifen-induced labeling of MG at 5 weeks of age, followed by immunohistochemistry analysis using the pan-RGC marker RBPMS at 4 weeks after AAV injection. IHC, immunohistochemistry.

(B) Total numbers of EYFP labeled MG examined in retinas receiving GFAP-tdTomato (an infection marker), together with GFAP-CasRx (control) or GFAP-CasRx-*Ptbp1* (*Ptbp1* downregulation).

(C) Total numbers of EYFP labeled MG that were also immunoreactive for the pan-RGC marker RBPMS per retina after *Ptbp1* downregulation.

(D-H) Confocal images showing expression of EYFP and RBPMS immunohistochemistry in retinas receiving GFAP-CasRx and GFAP-tdTomato.

(I-M) Confocal images showing expression of EYFP and RBPMS immunohistochemistry in retinas receiving GFAP-CasRx-*Ptbp1* and GFAP-tdTomato.

(D-M) Scale bar, 100 μm . ONL, outer nuclear layer. INL, inner nuclear layer. GCL, ganglion cell layer.

(N-O) Confocal images showing no detection of EYFP-labeled axons in the optic nerve after *Ptbp1* downregulation. Experiments were independently repeated 6 times with similar results. Scale bar, 500 μm .

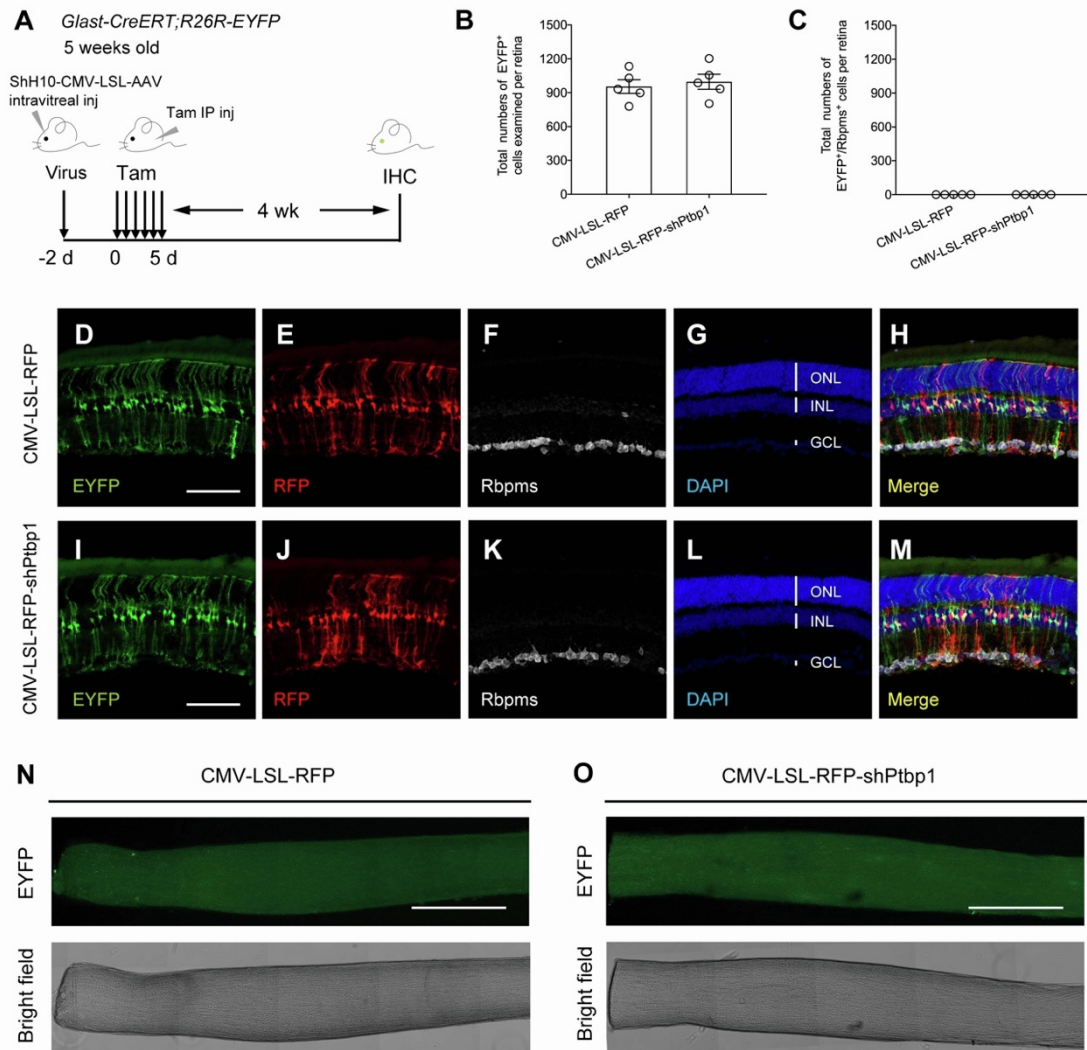


Figure S7. *Ptb1* downregulation by shRNA-based depletion fails to convert MG into RGCs in EYFP fate mapping (*Glast-CreERT;R26R-EYFP*) mice, related to Figure 3

(A) Experimental design for testing MG-to-RGC conversion in EYFP fate mapping mice. Intravitreal injection of ShH10-CMV-LSL-AAVs were performed in EYFP fate mapping mice at 5 weeks of age, followed by tamoxifen administration 2 days later to induce EYFP expression in MG and *Ptb1* depletion.

Immunohistochemistry analysis was performed using the pan-RGC marker RBPMS at 4 weeks after tamoxifen injection. IHC, immunohistochemistry.

(B) Total numbers of EYFP labeled MG examined in retinas receiving CMV-LSL-RFP (control) or CMV-LSL-RFP-shPtbp1 (*Ptb1* depletion).

(C) Total numbers of EYFP labeled MG that were also immunoreactive for the pan-RGC marker RBPMS per retina after *Ptb1* depletion.

(D-H) Confocal images showing expression of EYFP and RBPMS immunohistochemistry in retinas receiving CML-LSL-RFP (control).

(I-M) Confocal images showing expression of EYFP and RBPMS immunohistochemistry in retinas receiving CMV-LSL-RFP-shPtbp1 (*Ptb1* depletion).

(D-M) Scale bar, 100 μ m. ONL, outer nuclear layer. INL, inner nuclear layer. GCL, ganglion cell layer.

(N-O) Confocal images showing no detection of EYFP-labeled axons in the optic nerve after *Ptb1* depletion. Experiments were independently repeated 5 times with similar results. Scale bar, 500 μ m.